MODELING OF DM1 POS AND LOAD PERFORMANCE+

R. J. Commisso, J.R. Boller, D.V. Rose,* S.B. Swanekamp,* J.M. Grossmann, P.F. Ottinger, B.V. Weber, F.C. Young, and G. Cooperstein
Pulsed Power Physics Branch, Plasma Physics Division
Naval Research Laboratory, Washington, DC 20375

ABSTRACT

In this paper, we study the performance of the plasma opening switch (POS) and electron-beam diode load on the DM1 pulsed power generator using the transmission-line circuit code BERTHA, the electron/photon-transport code CYLTRAN, and the 2-dimensional particle-in-cell (PIC) code MAGIC. The results suggest that of the 52 kJ required to be delivered to the load to account for the observed radiation, up to 75% is associated with current not flowing in the cathode. This non-cathode current cannot be explained by electron vacuum flow only, implying the presence of plasma. Further, the inferred experimental diode impedance, 11 Ω, is much higher than optimum. Assuming no change in the DM1 conduction current/time and POS performance, an optimum diode impedance of 2 Ω, and a POS-to-load inductance reduced by 75%, the analysis suggests that the load energy on DM1 can range from 54 kJ to 94 kJ, depending on how much non-cathode current reaches the load. The analysis also suggests that to obtain agreement between features of the measurements and calculations, the DM1 flow impedance (gap) must decay after opening and ions must be present in the vacuum transmission line between the POS and load. Understanding of the coupling between the POS and e-beam load remains incomplete.

INTRODUCTION

DECADE[1] is a proposed 9-MJ, modular pulsed power generator. One such module, DECADE Module 1 (DM1),[2] is now in operation with an electron-beam (e-beam) diode load. Each module uses a coaxial plasma opening switch[3] (POS) for power conditioning. In this paper, we analyze the performance of DM1 during a selected experimental series. The purpose of this work is to try to improve the understanding of POS/load coupling and to suggest ways to optimize the DM1 single shot performance. Three different tools are used in this study. The transmission line code BERTHA[4] is used for circuit modeling that links the pulsed power to the POS and, using physics-based circuit-element models for the POS and e-beam diode load, predict the energy coupled to the load (for the experiments considered here, there are no load-current and only indirect load-voltage measurements). The coupled electron/photon Monte Carlo transport code CYLTRAN[5] is used to link the measured radiation associated with the e-beam load to the energy delivered to the load. The 2-D PIC code MAGIC[6] is used to help understand the electron and ion flow between the POS and load that accompanies the POS opening.

A simplified representation of the DM1 circuit and an illustration of the front-end geometry are given in Fig. 1. An in-depth description of the DM1 circuit can be found elsewhere.[1,7] The front-end geometry shown in Fig. 1 was used in the selected DM1 experiments and, unless otherwise noted, in all the calculations that follow.

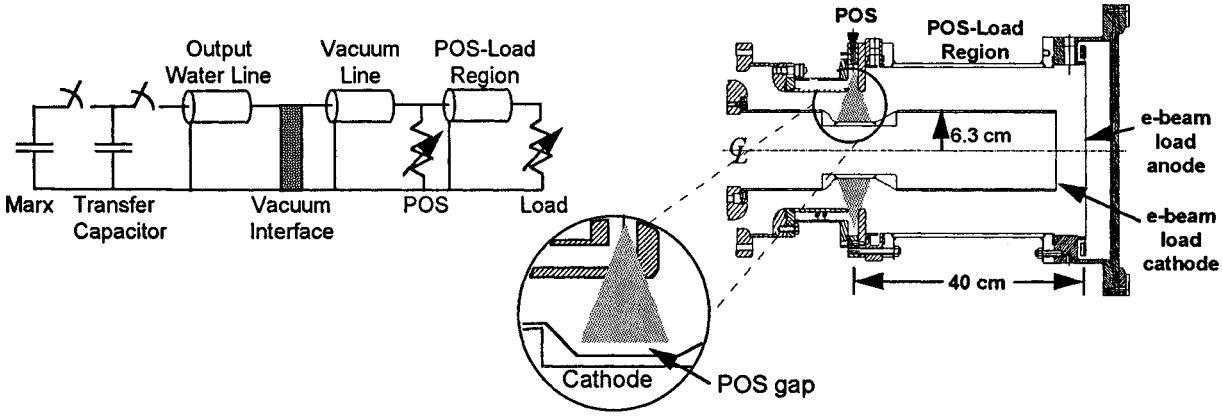

Fig. 1 Representation of the DM1 circuit and sketch of the front-end geometry used in the experiments.

Report Documentation Page

Form Approved
OMB No. 0704-0188

1. REPORT DATE	2. REPORT TYPE	3. DATES COVERED
JUL 1995	**N/A**	**-**

4. TITLE AND SUBTITLE
Modeling Of Dml Pos And Load Performance.

5a. CONTRACT NUMBER
5b. GRANT NUMBER
5c. PROGRAM ELEMENT NUMBER

6. AUTHOR(S)

5d. PROJECT NUMBER
5e. TASK NUMBER
5f. WORK UNIT NUMBER

7. PERFORMING ORGANIZATION NAME(S) AND ADDRESS(ES)
Pulsed Power Physics Branch, Plasma Physics Division Naval Research Laboratory, Washington, DC 20375

8. PERFORMING ORGANIZATION REPORT NUMBER

9. SPONSORING/MONITORING AGENCY NAME(S) AND ADDRESS(ES)

10. SPONSOR/MONITOR'S ACRONYM(S)
11. SPONSOR/MONITOR'S REPORT NUMBER(S)

12. DISTRIBUTION/AVAILABILITY STATEMENT
Approved for public release, distribution unlimited

13. SUPPLEMENTARY NOTES
See also ADM002371. 2013 IEEE Pulsed Power Conference, Digest of Technical Papers 1976-2013, and Abstracts of the 2013 IEEE International Conference on Plasma Science. Held in San Francisco, CA on 16-21 June 2013. U.S. Government or Federal Purpose Rights License.

14. ABSTRACT
In this paper, we study the performance of the plasma opening switch (POS) and electron-beam diode load on the DM1 pulsed power generator using the transmission-line circuit code BERTHA, the electron/photon-transport code CYLTRAN, and the 2-dimensional particle-in-cell (PIC) code MAGIC. The results suggest that of the 52 kJ required to be delivered to the load to account for the observed radiation, up to 75% is associated with current not flowing in the cathode. This non-cathode current cannot be explained by electron vacuum flow only, implying the presence of plasma. Further, the inferred experimental diode impedance, 11 n, is much higher than optimum. Assuming no change in the DMl conduction current/time and POS performance, an optimum diode impedance of 2 n, and a POS-to-load inductance reduced by 75%, the analysis suggests that the load energy on DMl can range from 54 kJ to 94 kJ, depending on how much non-cathode current reaches the load. The analysis also suggests that to obtain agreement between features of the measurements and calculations, the DMl flow impedance (gap) must decay after opening and ions must be present in the vacuum transmission line between the POS and load. Understanding of the coupling between the POS and e-beam load remains incomplete.

15. SUBJECT TERMS

16. SECURITY CLASSIFICATION OF:			17. LIMITATION OF ABSTRACT	18. NUMBER OF PAGES	19a. NAME OF RESPONSIBLE PERSON
a. REPORT	b. ABSTRACT	c. THIS PAGE			
unclassified	**unclassified**	**unclassified**	**SAR**	**6**	

RESULTS FROM CIRCUIT MODELING

The 48-element circuit model used in BERTHA for these circuit calculations has been successfully benchmarked against other models and successfully (within 10%) compared with measured DM1 electrical waveforms up to the POS.[7] Short descriptions of the circuit-element models for the POS and e-beam load as well as an example of the circuit modeling results follow. Details regarding the circuit-element models and benchmarking work, and complete circuit modeling results, can be found elsewhere.[7] We have assumed the full vacuum inductance for the region between the POS and load. This assumption is discussed later. The Marx charging voltage in the circuit calculations had to be reduced to 90% of the actual charging voltage in all of this work to obtain agreement with measurements.[7]

The circuit-element model for the POS is based on the concept of flow impedance,[8] where the resistance of the POS circuit element, R_S is related to the flow impedance, Z_f, by[7]

$$R_S = Z_f \left(\frac{I_{AU} + I_{CD}}{I_{AU} - I_{CD}} \right)^{1/2} \qquad (1)$$

Here, I_{AU} and I_{CD} are the anode current on the generator side (upstream) and cathode current on the load side (downstream) of the POS, respectively; R_S is the resistance of the POS ($R_S = V_S/I_S$, where V_S and $I_S = I_{AU} - I_{CD}$ are the POS voltage and current, respectively), and $Z_f \equiv V_S/(I^2_{AU} - I^2_{CD})^{1/2}$. In Eq. (1) we have also assumed that all the vacuum electron flow between the POS and load is lost and counted as switch loss. No vacuum electron flow is counted as current available for driving the e-beam load. The load current is I_{CD}. Because vacuum flow can contribute to the radiation produced in the experiment, we expect this POS circuit model to underestimate the load current. The biggest advantage of this model is that it allows one to differentiate between cathode and anode current reaching the load. However, Z_f still must be prescribed as a function of time. The physical model for the POS used in this work assumes that the vacuum electrons are always critically insulated (saturated flow) in the time dependent POS gap, D_{crit}.[3,7] If we further assume that the POS gap forms at the POS cathode radius, R_C, then one has that $Z_f \approx 30\ D_{crit}/R_C$.[9]

The circuit-element model[7] for the e-beam load is divided into three phases: 1) an early turn-on phase, 2) a Child-Langmuir (C-L) flow phase, and 3), a critical-current, pinched-beam phase. The model uses as input: the diode cathode outer radius, the cathode inner radius, the radius of curvature of the cathode edges, and the initial anode-cathode (AK) gap, D_d. The parameters for the load model are: the electric field turn-on threshold, the time duration to reach full C-L current, and the gap closure speed, v. In the first phase, the current begins to flow in the diode when the mean electric field reaches a preset threshold. Once the field threshold is exceeded, current rises linearly from zero to the full C-L value in the assumed diode "turn-on" time (during which plasma expands to cover the entire cathode area). In the second phase, the full C-L current flows and the diode AK gap closes from electrode plasma motion at a constant speed (closure is initiated at the start of "turn-on"). When the C-L current exceeds the critical current, the third phase begins which limits the diode current to the critical current for the remainder of the simulation. The critical current is expressed as

$$I_{CRIT} = 8500\ F_{CR} \frac{R}{D_d - vt} (\gamma^2 - 1)^{1/2} \ \text{(A)}, \qquad (2)$$

where F_{CR} is a factor that is weakly dependent on voltage and is approximately 1.6 for voltages between 1 and 3 MV, and γ is the ratio of electron energy to electron rest energy. The values of the diode parameters that best fit the DM1 data, and used here, are 10 kV/cm for the electric field turn-on threshold and 0 ns for the duration to full C-L current. Typical values of the electric field turn-on threshold and duration to full C-L current for similar diodes on the conventional water-line generators are 200-300 kV/cm and 10-20 ns, respectively. Long-conduction-time POS data from Hawk, where POS plasma may be in the e-beam load region at the time of opening, exhibit the same values as used here for DM1.[10] For all of this work, the closure speed was chosen to be 3.5 cm/μs, typical of similar diodes on water-line machines.

For the time dependence of Z_f in Eq.(1), we assumed a linear rise followed by an exponential decay.[7] This decay is needed to reproduce the measured upstream waveforms. We obtained a good fit to DM1 data when Z_f linearly increased to 1.38 Ω (maximum POS gap of about 2.3 mm) in 28 ns, then decreased exponentially (corresponding, e.g., to POS gap closure) with a 1/e time of 55 ns. Comparison of this model with the measured upstream waveforms from a DM1 shot is given in Fig. 2. Also shown in Fig. 2 is the calculated I_{AU} with a short circuit at the POS. It appears that the present DM1 operation utilizes only about 78% of this available current or

about 60% of the available stored energy if the POS conducted the entire current pulse. Displayed in Fig. 3 are the calculated load-voltage, V_L, and load-current, I_L, waveforms along with measured and calculated (using IV and $IV^{2.8}$ as approximations) x-ray signals. We do not have measured electrical load waveforms to compare with these calculations: however, the peak load voltage of 1.7 MV (inferred from a multi-channel, filtered PIN detector array[11]) agrees with the calculation. The AK gap of 25.4 mm used in the experiment corresponds to a load impedance of $Z_L = 11\ \Omega$. The calculated peak I_L is 150 kA and the load energy reaches 12.4 kJ when the measured x-ray pulse reaches zero.

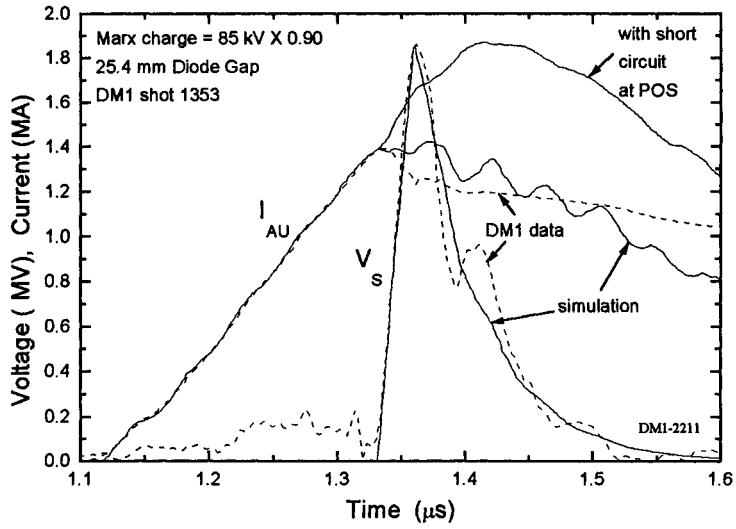

Fig. 2 Comparison of measured and calculated upstream waveforms.

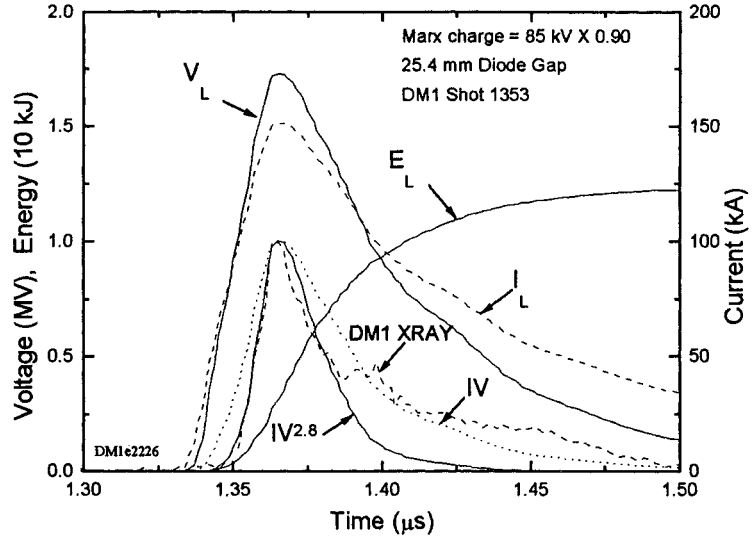

Fig. 3 Calculated load parameters and measured x-ray signal.

RESULTS FROM CYLTRAN MODELING

A full description of the e-beam diode geometry depicted in Fig. 1 and used in the CYLTRAN simulations, as well as detailed results of the radiation calculations, can be found elsewhere.[12] Briefly, the 12.7-cm radius Ta used as an anode in the e-beam diode was 0.003-in thick and the vacuum window was a 3/16-in thick sheet of polyethylene followed by a 3/4-in slab of polyethylene. The e-beam cathode radius of 6.35 cm was assumed to be the e-beam radius. The incident e-beam angular distribution was forward directed. The calculated dose-area-product (DAP) in the near field is relatively insensitive to this distribution.

Figure 4 contains a plot of the CYLTRAN-calculated DAP in 20 mils of Si as a function of diode energy for a variety of cases. The horizontal line at 7.6 Mrad (Si)-cm^2 is the average measured DAP for the chosen DM1 data set. The standard deviation, maximum, and minimum DAP values are also shown. The open symbols are CYLTRAN calculations for triangular-voltage, flat-current load waveforms. For the circles, the voltage is fixed at 1.75 MV and the current is varied to generate the linear scaling of calculated DAP as a function of load energy. For the two types of triangles, the current is held fixed at either 0.6 MA or 1.2 MA and the voltage is varied between 1 and 2 MV. Note that for these geometries the DAP is an approximately linear function of load energy. This result means that electrical energy delivered to the diode is a good parameter for optimizing radiation production. The filled squares are calculated DAPs for various BERTHA-generated load waveforms.[7] The point labeled "$D_{crit}(t)$ model" corresponds to prescribing Z_f in Eq. (1) by calculating $D_{crit}(t)$ from a form of Eq. (2) using the measured upstream waveforms and setting $Z_f = 30\ D_{crit}/R_C$.[7] The point marked "100 ns" is the result when only the energy in the first 100 ns of the calculated power pulse is used. More energy is delivered to the load when the AK gap and switch-to-load inductance, L_{SL}, are reduced because the present system is not optimized from a circuit point of view (see next section). The CYLTRAN results for the BERTHA waveforms fall on the same line

as the idealized waveforms, indicating that the DAP in 20 mils of Si for this configuration is relatively insensitive to the shape of the voltage and current waveforms.

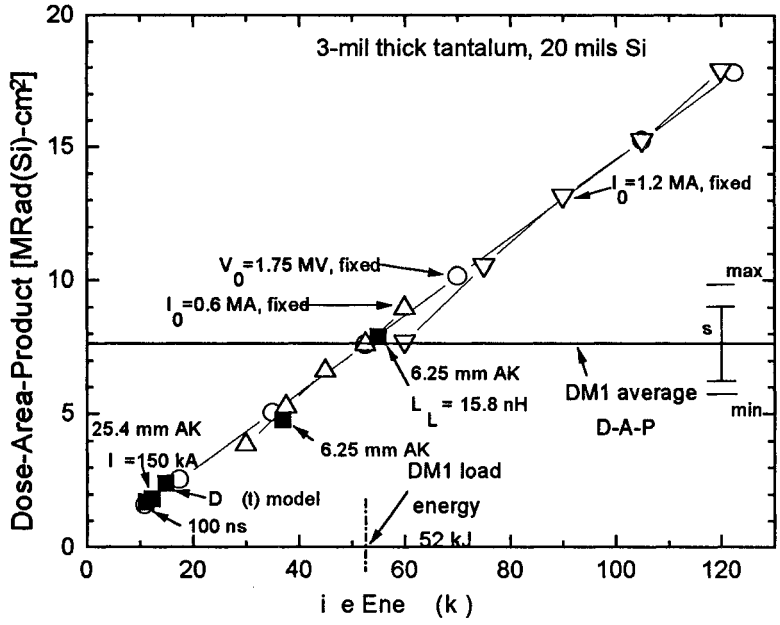

Fig. 4 Dose-area-product as a function of diode energy.

The energy at which the calculated DAP vs. load energy curve intersects the average measured DAP is the energy we infer is producing the observed DAP on DM1 - about 52 kJ. The BERTHA calculation underestimates the energy delivered to the load by approximately 40 kJ. The circuit-element model for the POS assumes only current flowing in the metal cathode, 150 kA peak, reaches the load. Thus we conclude that in the experiment, up to 40 kJ of energy associated with non-cathode current, 525 kA (assuming the experimental load power pulse waveform is comparable with the calculated one), reaches the anode and makes radiation. Electron vacuum flow alone cannot explain this result (see below). Note that comparisons of measured[11] and calculated radial dose profiles suggest that many electrons hit the anode at a radius well outside the e-beam cathode radius, supporting our conclusion that non-cathode current is present in the experiment.

RESULTS FROM VARYING CIRCUIT PARAMETERS

Several BERTHA runs were made varying D_d and L_{SL} from 25.4 mm and 63 nH to 5 mm and 15.8 nH, respectively (the former values being the ones used in the experiments).[7] These calculations show that the energy delivered to the load has a broad maximum of 37 kJ when D_d is about 6.3 mm, with an associated Z_L of about 2 Ω. This optimization was expected based on the critical gap picture of POS opening, where the optimum load impedance for maximum energy delivery to the load defines the boundary between switch-limited and load-limited operation.[3]

If L_{SL} is reduced, the load energy is also increased, but only if the load impedance is near the optimum impedance. If Z_L is large compared to the optimum Z_L, the beneficial effect of reducing L_{SL} is negated. For example, with D_d = 25.4 mm, there is no change in the energy delivered to the load as L_{SL} is reduced. This is because Z_L is so large (11 Ω) it dominates the inductive loading (approximated by L_{SL}/t_{open}, about 2 Ω for L_{SL} of 63 nH and t_{open} of 28 ns). Z_L of about 2 Ω is comparable to the maximum inductive loading and the system can deliver more energy to the load as L_{SL} is reduced. When D_d = 6.3 mm and L_{SL} = 15.8 nH (25% of the original vacuum inductance), we calculate that 54 kJ is delivered to the load. If we conjecture that the 40 kJ of load energy associated with the non-cathode current is still delivered to the load, then up to 94 kJ (upper bound) might be delivered to the load with this front-end configuration. The real system response must be determined experimentally.

RESULTS FROM 2-D PIC MODELING

To gain insight into the details of the POS-load coupling, we carried out preliminary 2-D PIC calculations of the behavior of the ion and electron flows using MAGIC. The DM1 front-end geometry (see Fig. 1) was used with the POS modeled by independently moving ions out of a prescribed gap in a prescribed time, as described previously.[9] For the results shown here, the final gap was 1.8 mm and the time for ions to clear the gap was 30 ns. This model, together with a simplified driving circuit, gave a good match to the upstream DM1 waveforms. POS plasma was modeled by allowing ion emission along both sides of the POS. The load for the simulation was an e-

beam diode with no ions, an electric field threshold for electron emission of 100 kV/cm, and a 25-mm AK gap. The full DM1 current flowed in the circuit upstream of POS at time t=0 (initiation of opening).

Measurements on Hawk with downstream current monitors in the anode and cathode suggest that the current propagates to the load nearer the anode first with a speed of the order of 1000 cm/μs, followed by current flowing in the cathode.[13] Recent results from DM1 show similar behavior. On Hawk, the time delay between the current measured near the load and at the anode and the initiation of cathode current flowing, as well as the ratio of anode to cathode current, decrease with decreasing Z_L. Several possible mechanisms have been proposed to explain the process of current transfer to the load including: vacuum electron flow, electron migration along the downstream anode via plasma production at the anode,[14] and various scenarios involving electron-propagation/current-transport through or by a downstream plasma. In the simulations described here, there is no attempt to include plasma that may be in the POS-to-load region as a result of the POS plasma injection and/or the conduction process. Also, there was no self-consistent algorithm for producing ions at the anode from electron energy deposition. Within the context of these assumptions, the POS-to-load inductance is self-consistently accounted for in the PIC simulations.

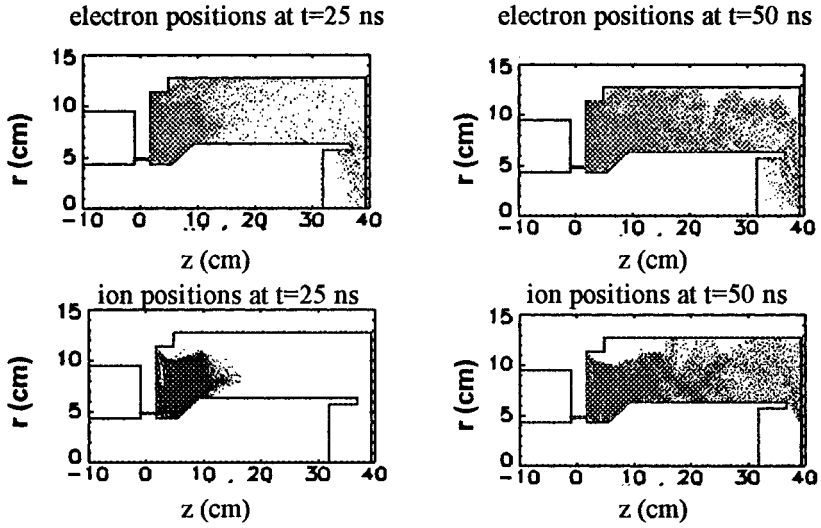

Fig. 5. Electron and ion positions at two times after opening.

In Fig. 5, ion and electron positions are plotted at two different times. At t=25 ns, the electrons fill the downstream region and drag ions associated with the POS plasma into the vacuum line between the POS and load. At t=50 ns, the ions (plasma) also fill the vacuum line. The behavior of the particle flow is distinctly different from that reported in previous simulations,[9] where the electrons hugged the anode of the vacuum line between the POS and load. In this case, the electron flow is more uniformly distributed in radius. The cause of this discrepancy is under investigation. The onset of significant (anode) current in the diode is associated with the arrival of plasma to the diode. The speed with which the plasma moves depends on the ratio of ion charge to atomic number, Z/A, which for this simulation was assumed to be 2/5 (corresponding, e.g., to an 18% C^{++}/82% H^{+} plasma - by comparison, purely C^{++} ions would have Z/A=2/12). This Z/A was chosen to have the anode current and load power peak near the expected time after opening. The cathode current predicted by this simulation is close to the 150 kA predicted by the circuit modeling. Also, the sequencing of anode and cathode monitors observed on Hawk[13] and DM1 is qualitatively reproduced, with the speed of propagation about 1000 cm/μs. However, the total current reaching the load in the simulation was only 200 kA, a factor of 3.5 lower than what was inferred above from the radiation measurements. With a Z/A of 2/12, the total load current is less than 150 kA. These results will depend on the plasma Z/A and the existence of other plasma, either injected into or generated in the vacuum line. For example, in a recent simulation ion emission was allowed along the anode (treated as a zero work function ion source) between the POS and load. This resulted in a peak load current of 450 kA, a closer match to the inferred load current, but with the current beginning 15 to 20 ns too early. Here, a model for anode plasma production based on local energy deposition is needed. Additional simulations along with better measurements of plasma density are required to more fully understand the POS/load coupling.

SUMMARY

We have performed an analysis of a selected set of data from the DM1 pulsed power generator using the transmission-line circuit code BERTHA, the electron/photon-transport code CYLTRAN, and the 2-dimensional particle-in-cell-code MAGIC. The results suggest that up to 75% of the energy delivered to the diode is associated with non-cathode, radiation-producing current. For the experimental series considered, the system is not optimized for energy delivery to the load. The diode impedance of 11 Ω is much higher than optimum. With the

same DM1 conduction current/time and POS performance considered in this paper, an optimum diode impedance of 2 Ω, and a POS-to-load inductance reduced by 75%, this analysis suggests the load energy on DM1 can range from 54 kJ to 94 kJ, depending on how much non-cathode current reaches the load. To obtain agreement between features of the measurements and calculations, the DM1 flow impedance (gap) must decay after opening and ions must be present in the vacuum transmission line between the POS and load. While progress has been made in describing the coupling between the POS and e-beam load, both experimental and theoretical work is required for a fuller understanding of this complex process.

The authors wish to thank Drs. J. Goyer and D. Kortbawi of Physics International for generously giving of their time in providing DM1 data and information on the DM1 operation, Dr. R. Adler for his help in starting and interpreting the CYLTRAN calculations, and Dr. J. Rowley of the Defense Nuclear Agency for his support in this effort.

+ Work Supported by the Defense Nuclear Agency.
* JAYCOR, Inc., Vienna VA.

REFERENCES

1. "The DECADE High Power Generator," P. Sincerny, S. Ashby, K. Childers, C. Deeney, D. Drury, J. Goyer, D. Kortbawi, I. Roth, C. Stallings, and L. Schlitt, in Proceedings of the 9th IEEE International Pulsed Power Conference, R. White and W. Rix, eds., San Diego, CA (1993), IEEE Cat. No. 93CH3350-6, p. 880.
2. "Performance of DECADE Module #1 (DM1) and Status of the DECADE Machine," P. Sincerny, S. Ashby, K. Childers, J. Goyer, D. Kortbawi, I. Roth, C. Stallings, J. Dempsey, and L. Schlitt, in Proceedings of this Conference, W. Baker and G. Cooperstein, eds., Albuquerque, NM (1995), paper 12-3.
3. "Characterization of a Microsecond-Conduction-Time Plasma Opening Switch," R.J. Commisso, P.J. Goodrich, J.M. Grossmann, D.D. Hinshelwood, P.F. Ottinger, and B.V. Weber, Phys. Fluids B 4, 2368 (1992); and references therein.
4. "BERTHA - A Versatile Transmission Line and Circuit Code," D.D. Hinshelwood, NRL Memorandum Report 5185, (Nov. 1983), unpublished.
5. "ITS: The Integrated TIGER Series of Electron/Photon Transport Codes - Version 3.0," J.A. Halbleib, R.P. Kensek, G.D. Valdez, S.M. Seltzer, M.J. Berger, IEEE Trans. Nucl. Sci. NS-39, 1025 (1992).
6. "User Configurable MAGIC for Electromagnetic PIC Calculations," B. Goplen, L. Ludeking, D. Smithe, and G. Warren, Comp. Phys. Comm. 87, 54 (1995).
7. "Circuit Simulations of DM1 with an Electron-Beam Load," R.J. Commisso, J.R. Boller, D.V. Rose, and S.B. Swanekamp, NRL Memorandum Rep. 7750 (March 1996), unpublished.
8. "Experiments on a Current-Toggled Plasma-Opening Switch," C.L. Mendel, Jr., M.E. Savage, D.M. Zagar, W.W. Simpson, J.W. Grasser, and J.P. Quintenz, J. Appl. Phys. 71, 3731 (1992).
9. "Power Flow between a Plasma-Opening Switch and a Load Separated by a High Inductance Magnetically Insulated Transmission Line," S.B. Swanekamp, J.M. Grossmann, P.F. Ottinger, R.J. Commisso, and J.R. Goyer, J. Appl. Phys. 76, 2648 (1994).
10. "Modeling the Hawk POS with a Diode Load," J.R. Boller, R.J. Commisso, and B.V. Weber, Pulsed Power Physics Branch Technote No. 95-17 (1995), unpublished.
11. J. Goyer and D. Kortbawi, personal commumication.
12. "Bremsstrahlung Yield Simulations for DM1," D.V. Rose, R.J. Commisso, S.B. Swanekamp, and F.C. Young, NRL Memorandum Report 7748 (Nov. 1995), unpublished.
13. "Review of Hawk Power Flow Experiments," B.V. Weber, R.J. Commisso, P.J. Goodrich, J.M. Grossmann, S.B. Swanekamp, P.F. Ottinger, and R.A. Riley, presented at the DNA Opening Switch Workshop, NSWC, Silver Spring, MD, March (1995), Pulsed Power Physics Branch Technote No. 95-12 (1995), unpublished.
14. "Experimental and Theoretical Investigation of 2-D Power Flow," S.B. Swanekamp, J.R. Boller, R.J. Commisso, D.D.Hinshelwood, P.F. Ottinger, and D.V. Rose in Proceedings of this Conference, W. Baker and G. Cooperstein, eds., Albuquerque, NM (1995), paper P2-21.